





Microplasma spraying of coatings from wire of heat-resistant nickel alloy Inconel 82 with laser melting

Volodymyr Korzhyk^{1,2}, Shiyi Gao^{1*}, Vladyslav Khaskin^{1,2},
Artemyi Bernatskyi², Oleksandr Kislitsya², Sergyi Voinarovych²,
Yevhenii Kuzmych-Yanchuk², Sergyi Kaluzhnyi², Yanchao Hu², Guirong²

¹ Guangdong Provincial Key Laboratory of Material Joining and Advanced Manufacturing, China-Ukraine Institute of Welding, Guangdong Academy of Sciences, Guangzhou, 510650, China

² E.O. Paton Electric Welding Institute, National Academy of Sciences of Ukraine. 11 Kazymyr Malevych Str., Kyiv, 03150, Ukraine

* Corresponding author's e-mail: meshiyigao@163.com

ABSTRACT

The work is devoted to studying the technological capabilities of the processes of microplasma spraying of wires from heat-resistant nickel alloy Inconel 82 with further laser melting of the sprayed layers to produce narrow-path coatings during restoration of worn end faces of ribbed parts, used in nuclear engineering, aerospace and textile industry, etc. Numerical modeling by finite element method was applied to select the parameters of the modes of microplasma wire spraying and further laser melting of sprayed layers of Inconel 82 alloy. This made it possible to select the parameters of the modes with an accuracy of up to 20% (current 30–40 A at voltage 40 V, deposition speed 100 mm/min; radiation power 3.0 kW, defocusing spot 3 mm, remelting speed 750 mm/min). The value of the parameter of coating growth rate during microplasma spraying of Inconel 82 alloy wire was determined (it was equal to 1 mm of coating height / 1 cm of narrow path length / 1 min of spraying process duration). The work shows for the first time that the useful area of the microplasma spraying spot is close to the defocused laser radiation spot, ensuring unique possibilities for deposition of narrow paths and their laser remelting without hard phase burnout. This is experimentally confirmed by ~17% (290–350 HV) increase in the hardness of sprayed Inconel 82 layer (200–240 HV) during its remelting by radiation with power density of $\sim 4.3 \cdot 10^4$ W/cm². It was also determined that the features of structure formation during laser remelting of Inconel 82 alloy promote an enhancement of its corrosion resistance up to 1.5 times and increase in wear resistance by 20–40%, compared to sprayed coatings.

Keywords: microplasma spraying, wires, Inconel 82 alloy, adhesion strength, laser melting, microstructures, defects, microhardness.

INTRODUCTION

During selection of the restoration processes and development of modern repair technologies, plasma technologies attract significant interest of researchers. They have become widely accepted in medicine, power engineering, mechanical engineering, tool and textile production, instrument making and other industries [1, 2]. These technologies allow strengthening the part working surfaces and restoring them after wear [3, 4]. However, application of modern industrial

plasma units, usually having the power from 30 to 60 kW [5, 6] for coating deposition on products with wall thickness below 1–3 mm, is related to the risk of local overheating and deformation of both the parts and the coatings proper [7, 8]. Another technological feature of application of plasmatrons of such a power is a rather large diameter of the spraying spot, being usually equal to 12–30 mm [9, 10]. When spraying small parts, narrow edges or paths (bands) it leads to significant spraying material losses and the need for

performing an additional operation of mask application on unsprayed areas [11, 12].

The E.O. Paton Electric Welding Institute developed a method of microplasma spraying of wire materials [13, 14]. This method is based on application of a plasma jet, generated by a plasmatron of up to 2 kW power at currents of 20–50 A. Spraying spot diameter is in the range of 1–5 mm. It allows deposition of narrow-path coatings, as well as restoring parts with worn narrow ribs without any significant loss of spraying material and without their overheating [15, 16]. Produced coatings have a wide functionality, making relevant the application of such a method of their deposition [17, 18].

The main problems of microplasma spraying of narrow-path coatings (both from powder and from wire materials) are formation of some internal porosity in them [19, 20] and the need for pre-treatment of the sprayed surface (for instance, gas-abrasive) to increase the strength of adhesion to the substrate [21, 22]. Both these problems can be solved by laser remelting of the sprayed layers [23, 24]. Additional advantages of the laser process can be an increase in the density and corrosion resistance of the produced coatings [25, 26]. Works on laser remelting of the layers produced by powder spraying, are already quite well-known (for instance, [27, 28]). Researchers have established that in laser remelting of pre-deposited (including sprayed) layers the action of surface tension forces in the melt pool results in metal drawing to the remelted bead axis, leading to significant undercuts between the remelted beads [29, 30]. One of the variants of elimination of this problem is spraying of single paths with subsequent formation of individual beads by laser remelting [31, 32]. This, however, may give rise to still another problem – sprayed coating delamination caused by laser remelting [33].

In addition to solving the above-mentioned general problems of laser remelting of the sprayed layers (for instance, [34, 35]), it is of interest to study remelting of such layers, which have been produced exactly by wire microplasma spraying [36, 37]. The process of wire plasma spraying proper has certain advantages. For instance, due to a certain increase in the size of NiAl particles, deposited on the substrate from stainless steel 304 and aluminium alloy 7075 by plasma spraying with wire feed, the adhesion strength can be increased to 82.67 ± 3.96 MPa and 64.45 ± 2.84 MPa, respectively [38]. One can anticipate that

wire plasma spraying will allow eliminating the drawback of coating delamination during subsequent laser remelting [39, 40].

Investigation of laser remelting of the layers sprayed using Inconels is of special interest [41, 42], as these alloys have a rather wide range of applications – from protection against corrosion to restoration of blades of gas turbine engines. In particular, interesting aspects of potential application of the technology of microplasma spraying of Inconels and other corrosion-resistant alloys with subsequent laser remelting can be structural elements of nuclear reactor fittings [43], solar power stations [44], functional surfaces of products subject to erosion, corrosion and cavitation [45], surfaces operating under the conditions of light or periodic wear [46], etc.

Thus, it is rational to apply laser remelting of the surface to increase the adhesion strength of the sprayed coating from Inconel type alloys to the substrate base metal. In order to eliminate the risk of sprayed coating delamination caused by laser remelting, it is rational to apply wire plasma spraying. Solving such a problem is related to determination of a complex of parameters, in particular, establishing the regularities of heat input influence on structure formation in the layers during spraying and subsequent remelting [47, 48].

PURPOSE, MATERIALS AND METHODS

The objective of the work was studying the technological capabilities of the processes of microplasma spraying of Inconel 82 alloy wires with further laser melting of the sprayed layers to produce narrow-path coatings at restoration of worn end faces of ribbed parts, applied in nuclear power engineering, aerospace and textile industry, etc. To achieve this goal, the following tasks were solved:

- selection of the parameters of the modes of microplasma wire spraying and further laser melting of sprayed layers of Inconel 82 alloy;
- microplasma spraying of coatings from Inconel 82 wire;
- laser melting of the deposited microplasma coatings from Inconel 82 alloy wire;
- metallographic investigations of the obtained results.

Wire 0.3 mm in diameter from Inconel 82 alloy was used as the spraying wire (Table 1) [49]. Spraying was performed on samples of

complex-alloyed steel of 24CrMoV55 type (or 25Kh2M1F, GOST 2591-2006) (Table 1) [50], which were plates of $50 \times 50 \times 10$ and $50 \times 3 \times 10$ mm size, as well as plates with artificially worn ribs ~ 3 mm wide and 3–8 mm high, milled out on their surface.

Procedure of work performance was as follows. Tentative parameters of the modes of microplasma wire spraying were selected based on performed calculations and available experience, in particular that described in the respective publications. Selected parameters were refined experimentally. Parameters of laser remelting mode were chosen based on calculations. Selected parameters were also refined experimentally. After that, microplasma wire spraying with Inconel 82 alloy with subsequent laser melting was performed on simulator-samples. Variants of spraying untreated surfaces and surfaces treated by gas-abrasive process were compared to establish the strength of sprayed layers adhesion to the base (stainless steel). Adhesion strength was determined by tearing off the deposited layers under static tension (Fig. 1). Sprayed and remelted layers were studied by metallographic methods using optical microscopy and microdurometric analysis.

Metallographic studies were conducted using optical microscope NEOPHOT-32 (CARL ZEISS, Jena, Germany) with application of the procedure of [51, 52]. To identify the microstructure of the samples, electrolytic etching was carried out with 20% water solution of ammonium hydroxide (chloride) at voltage $U = 6 \dots 8$ V during time $\tau = 4 \dots 6$ s [53]. Microhardness of Vickers samples was measured using M400 microhardness tester (LECO, St. Joseph, MI, USA) at 300 gs load, and the values of sample hardness were determined according to ISO 6507 (Metallic materials – Vickers hardness test – Part 1: Test method) and ASTM E384 (Standard Test Method for Microindentation Hardness (1–200 gf) of Materials to Vickers and Knoop) [54]. To evaluate the strength of adhesion

of the sprayed layers to the steel base, testing was carried out using a standard adhesive technique in a universal servo-hydraulic testing complex MTS 318.25 (MTS Systems Corporation, Eden Prairie, Minnesota, USA) with maximum force of 250 kN. To determine the wear resistance of the sprayed and remelted layers of Inconel 82 alloy, a grinding machine 2070 SMT-1 was applied with a “disc-pad” pattern, using a bronze disc and pad made of steel 24CrMoV55 with sprayed (remelted) coating from Inconel 82 [55, 56].

SELECTION OF THE MODES OF SPRAYING AND FURTHER MELTING OF INCONEL 82 ALLOY LAYERS

For preliminary selection of the parameters of microplasma wire spraying and further laser melting of the sprayed layers, calculations were performed using approaches proposed in [57–63].

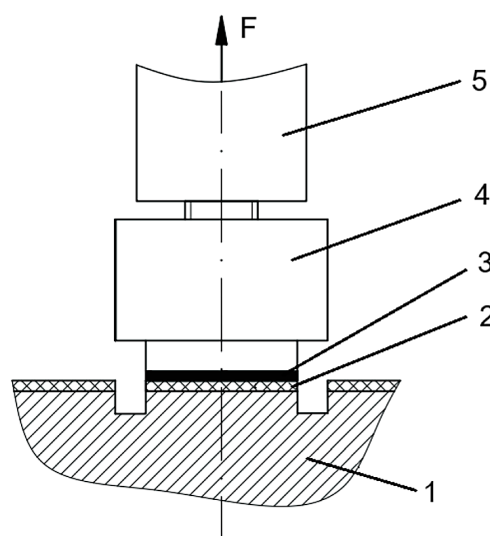


Figure 1. Scheme of testing the adhesion strength of a sprayed coating to a base: 1 – sample; 2 – coating; 3 – adhesive (glue); 4 – counter-sample; 5 – equipment of the MTS 318.25 testing machine

Table 1. Composition of materials used in the investigations

| Material | Element Content, wt. % | | | | | | | | | | |
|-------------------|------------------------|-----|-----------|-----------|---------|--------|---------|-------|---------|---------|-------------------------|
| | Fe | B | C | Si | Mn | Ni | Cr | Cu | P | S | Other |
| Substrate metal | | | | | | | | | | | |
| 24CrMoV55 steel | Base | – | 0.22–0.29 | 0.17–0.37 | 0.4–0.7 | < 0.25 | 2.1–2.6 | < 0.2 | < 0.03 | < 0.025 | Mo < 0.9–1.1 V < 0.5 |
| Filler materials | | | | | | | | | | | |
| Inconel 82 (wire) | < 3.0 | 0.1 | < 0.04 | < 0.5 | < 2.9 | Base | 19.0 | – | < 0.001 | < 0.001 | Nb < 2.25 Ti < 0.5 |

Heat input into the base metal (steel plate) and laser penetration depth were calculated by the equation of heat transfer in a plate being melted, in the following form [57]:

$$C(T)\rho(T)\frac{\partial T}{\partial t} = \frac{\partial}{\partial z}\left(\lambda(T)\frac{\partial T}{\partial z}\right), \quad (1)$$

$$0 < z < H, t > 0$$

where: $C(T)$, $\rho(T)$, $\lambda(T)$ are the effective heat capacity of the metal (taking into account the latent heat of melting), density and thermal conductivity coefficient, respectively; z is the vertical coordinate of heat distribution in the system of “remelted Inconel 82 coating (of thickness h) – 24CrMoV55 plate (of thickness H), onto which the coating is sprayed”; t is the time of heat propagation along the coordinate z , which is the ratio of the length of the heat source in the remelted layer to the speed of movement of this source.

For calculation according to dependence (1), we assume that at the interface of the sprayed layer of Inconel 82 and steel 24CrMoV55 (at $z=h$) conditions of ideal thermal contact are in place [57]:

$$T(h-0, t) = T(h+0, t);$$

$$\lambda \frac{\partial T}{\partial z}\bigg|_{z=h-0} = \lambda \frac{\partial T}{\partial z}\bigg|_{z=h+0} \quad (2)$$

We will take the boundary conditions for Equation 1 as [57]:

$$\frac{\partial T}{\partial z}\bigg|_{z=H} = 0; -\lambda(T)\frac{\partial T}{\partial z}\bigg|_{z=0} =$$

$$= q - q_r - q_{ev} \quad (3)$$

where: q is the heat flow that is applied to the system of “Inconel 82 coating (of thickness h) – 24CrMoV55 plate (of thickness H)”; q_r is the heat flow lost due to thermal radiation emitted from the heating zone; q_{ev} is the heat flow lost due to evaporation.

First finite element method, using dependencies (1)–(3), was applied to calculate the heat input into the steel plate during microplasma spraying, which occurs due to the impact on the plate of an indirect plasma jet with molten Inconel 82 particles (Fig. 2). In the selected variant, plasma-tron movement with the speed of 200 mm/min at the power of 1.2–1.6 kW without allowing for process efficiency, or 0.6–0.8, allowing for efficiency at the level of 50%. The power applied to the base metal is up to 100 W.

Recommendations from published sources, in particular work [59, 60], were used for further refining of the parameters of the modes of microplasma wire spraying. According to these studies, current $I = 30\text{--}40$ A should be used for spraying wires 0.3 mm in diameter from materials close to Inconel 82, with plasma forming gas flow rate close to 3 l/min and shielding gas flow rate of the order of 5–8 l/min. Such mode parameters will allow spraying the respective metal wire, fed at the speed $W = 3\text{--}6$ m/min, and performing spraying at a distance of 60–120 mm. As a result, coatings from 1.0–1.2 to 1.8–2.0 mm high can be sprayed with the plasma-tron movement speed of 100–200 mm/min.

After that, temperature distribution was calculated by the depth of the system of remelted Inconel 82 coating – 24CrMoV55 plate, on which

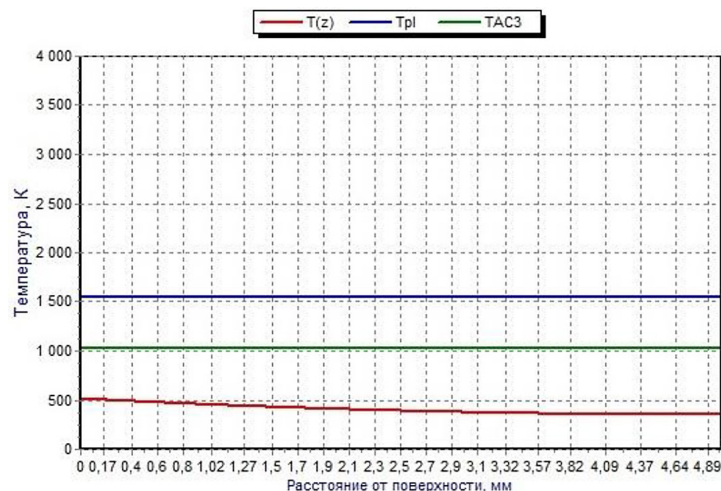


Figure 2. Distribution of temperature T over depth z of 24CrMoV55 plate during microplasma spraying of Inconel 82 coating

coating was deposited, based on dependencies (1)–(3), using the finite element method (Fig. 3). Performed calculation showed that the guaranteed remelting of coatings up to 1.2 mm thick to a somewhat greater depth (of the order of 1.3–1.4 mm) occurs at movement of 3.0 kW laser radiation, defocused into a spot 3.0 mm in diameter, with the speed of 750 mm/min.

DEVELOPMENT OF AN EXPERIMENTAL UNIT AND SAMPLE PREPARATION

Proprietary experimental unit MPN-004 was used for microplasma deposition of coatings from

Inconel 82 alloy wire (Fig. 4). This unit includes inverter power source Master TIG 200 P (Kemp-pi OY Company, Finland) with control panel 1, block of gas flow rate and wire feed rate control 2, independent cooling block 3, microplasmatron 4, wire feeder 5, cylinder with argon 6. Spraying was performed using a linear sample mover, mounted in a fume hood. Table 2 gives the main characteristics of MPN-004 unit.

Nd:YAG-laser of DY 044 model (ROFIN-SINAR Laser GmbH, Germany) with up to 4.4 kW radiation power was used for laser remelting of the sprayed layers of Inconel 82 alloy. Remelting was also performed using a linear mover. Deposition of Inconel 82 coating was performed in

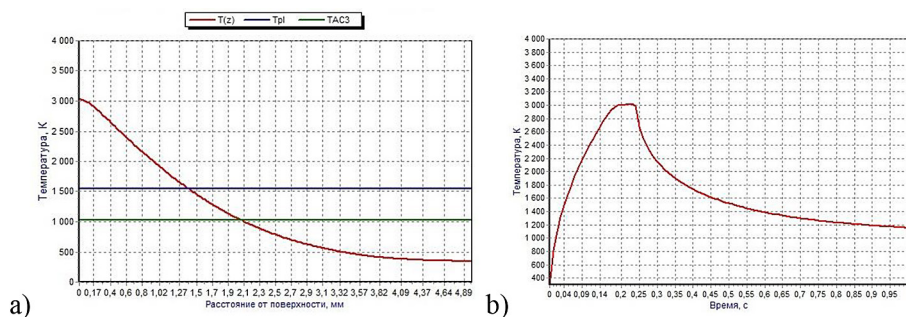


Figure 3. Distribution (a) of temperature T over depth z of system of “remelted Inconel 82 coating – 24CrMoV55 plate, on which coating was deposited” and thermal cycle (b) of laser remelting process (T_m – melting temperature)

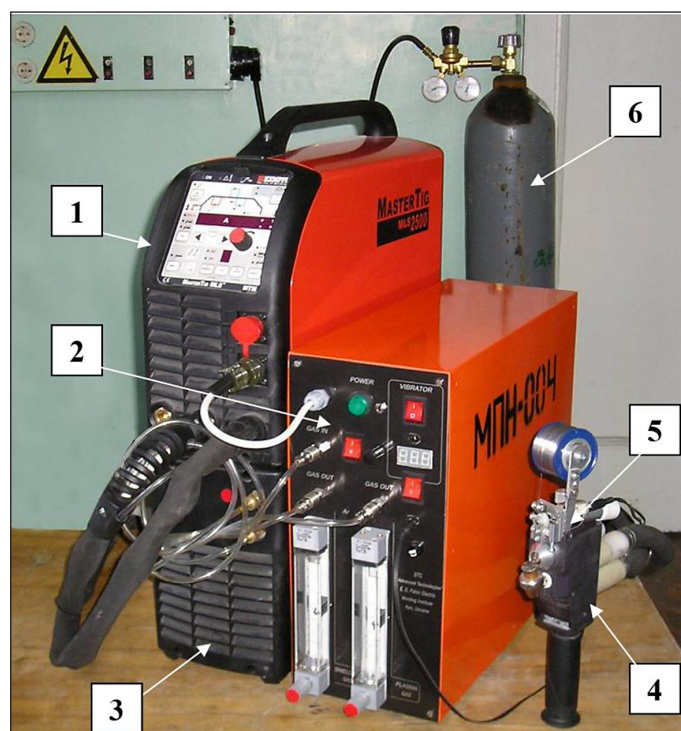


Figure 4. Appearance of MPN-004 unit

Table 2. Main technical characteristics of MPN-004 unit

| | |
|-------------------------------------|-----------------|
| Working gas | Argon |
| Shielding gas | Argon |
| Plasma jet power, kW | Up to 3.0 |
| Current, A | 10...60 |
| Voltage, V | 20...50 |
| Plasma forming gas flow rate, l/min | 0.5...5 |
| Shielding gas flow rate, l/min | 2...10 |
| Productivity, kg/h | 0.1...2.5* |
| Material Usage Ratio, % | 0.6...0.9* |
| Overall dimensions, mm | 500 × 360 × 650 |
| Weight, kg | 44 |

Note: * At spraying of coatings from powders.

the form of paths, sprayed on the surface of $50 \times 50 \times 10$ mm 24CrMoV55 steel plates, as well as on the longitudinal end face of $50 \times 3 \times 10$ mm plates to produce narrow beads 3 mm wide. Milling of $50 \times 50 \times 20$ mm plates was also performed to produce ~3 mm wide and 3–8 mm high ribs on their surface. Local depressions were made on these ribs, which simulated the worn defective

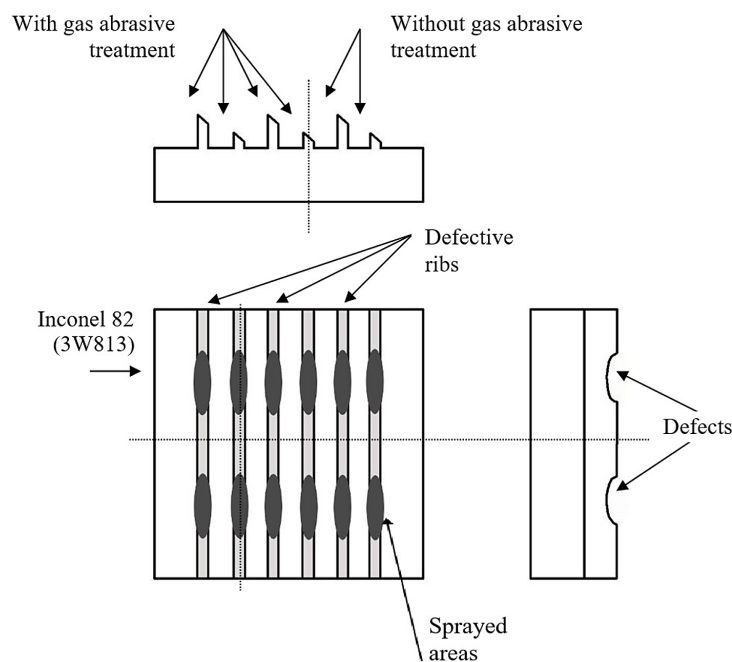
zones, which were further on restored by spraying with subsequent remelting (Fig. 5).

INVESTIGATION RESULTS

Microplasma spraying of coatings from Inconel 82 wire

To finally determine the parameters of microplasma spraying of Inconel 82 alloy wire, a series of experiments were conducted, which were based on the above parameters chosen from publications. In these experiments, a coating from Inconel 82 alloy wire was applied in the form of narrow paths on flat samples from 24CrMoV55 steel of $50 \times 50 \times 10$ mm size. As a result, parameters of modes No. 1 and No. 2, given in Table 3, were selected. Two narrow paths 2–3 mm wide were deposited on some samples, according to these modes, in order to determine the sprayed layer height (Fig. 6).

Experiments were also performed on microplasma wire restoration of profiles of samples

**Figure 5.** Schematic representation of samples with indication of zones for rib profile restoration (rib width is ~3 mm)**Table 3.** Parameters of microplasma wire spraying of coatings from Inconel 82 alloy wire on 24CrMoV55 steel

| Mode No. | Spraying current I, A | Plasma forming gas flow rate, Q, l/min | Distance L, mm | Spraying speed V, mm/min | Wire feed rate W, m/min. | Sprayed coating height h, mm |
|----------|-----------------------|--|----------------|--------------------------|--------------------------|------------------------------|
| 1 | 40 | 2.82 | 100 | 100 | 3.4 | 1.0–1.2 |
| 2 | 30 | 3.0 | 60 | 100 | 5.8 | 1.7–1.9 |

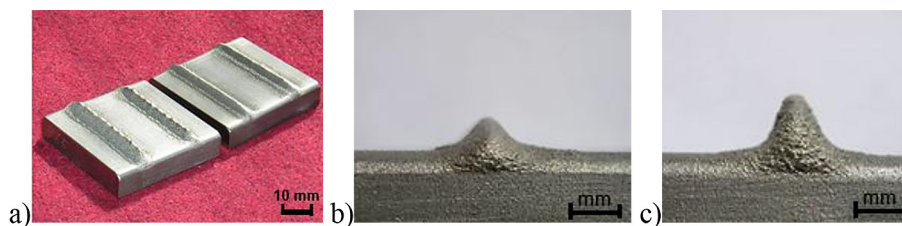


Figure 6. Appearance of samples (a) and narrow paths from Inconel 82 sprayed in mode No. 1 of 1.0–1.2 mm height (b) and in mode No. 2 of 1.7–1.9 mm height (c)

with artificially worn ribs, according to the schematic, given in Figure 5. In this case, coatings were sprayed in the zones of artificial wear (depression) so that the sprayed metal spread also to the unworn rib surface. Figure 7 gives the appearance of the sprayed samples.

As one can see from Figure 7, microplasma spraying method allows rather accurately restoring the geometrical shape of worn parts that significantly reduces the scope of further machining operations.

Laser processing of applied microplasma coatings from Inconel 82 alloy wire

Experiments on laser processing of microplasma wire coatings from Inconel were conducted. The objective of the experiments was assessment of the effectiveness of such processing to increase the strength, density and mechanical properties of the coatings.

Processing of sprayed coatings was performed using Nd:YAG-laser of DY 044 model

(ROFIN-SINAR, Germany) with up to 4.4 kW radiation power. Laser processing parameters were as follows: 3.0 kW power, ~3.0 mm diameter of radiation spot, 750 mm/min processing speed. Ar was used for protection of the processing zone. General view of the remelted coating is given in Figure 8.

Metallographic studies of the obtained results

General view and microstructure of Inconel 82 coatings, deposited on narrow sides of the samples (6 and 3 mm) before and after laser processing are shown in Figures 9–10. In Figure 9a it is evident that there is a clearly defined interface between the deposited layer and the substrate. After laser remelting (Fig. 9b) this interface becomes significantly less clearly defined. According to paper [31] this may indicate the formation of a metallurgical bond between the remelted layer and the substrate.

Metallographic studies of the cross-sectional microstructure of a bead formed as a result of microplasma spraying in mode 1 (Table 3) showed that its height reaches 1.25 mm, and its width is 4 mm during spraying of the surface of a sample 6 mm wide (Fig. 9,a and 10,a). During spraying of 3 mm wide samples in the same mode, the bead



Figure 7. Appearance of a sample with defective zones, restored by microplasma wire spraying



Figure 8. Appearance of the sample after laser remelting of the coating

width corresponded to sample width. A bead deposited in mode 2 was selected for laser remelting (Table 3). After remelting, this bead becomes narrower due to the action of surface tension forces, and its height and width are 2.0 and 2.6 mm, respectively (Fig. 9b and 10b).

In an unetched state, a slight porosity of 3–5% is observed in the microplasma sprayed layers (according to ASTM E2109-01(2021) Standard Test Methods for Determining Area Percentage Porosity in Thermal Sprayed Coatings). Fine oxide inclusions and delaminations from the base 1.4 mm long are observed in the zone of sprayed coating bonding with the base metal.

A fine lamellar structure of the bead is identified as a result of etching. The lamelle form factor is up to 14–20 (width to thickness ratio). Particles of a spherical shape 30–50 μm in diameter

and semi-spherical shape of 30–40 μm radius are sometimes observed (Fig. 11). During microhardness measurement it was found that the spray-deposited bead from Inconel 82 alloy has average microhardness of 218 ± 15 HV. Average microhardness of the steel base is equal to 339 ± 4 HV. No changes in the steel structure in the joint zone are observed visually, and the microhardness does not differ from that of the base metal and is equal to ~ 341 HV. At the bottom of Figure 11a the interface between the sprayed layer and the substrate is clearly visible. Detailed studies of this interface showed that it contains oxides and silicides of nickel and iron. This may indicate a low level of adhesion.

After laser remelting the bead metal changed its shape and became close to a semi-sphere in its cross-section (Fig. 9b). No porosity is observed

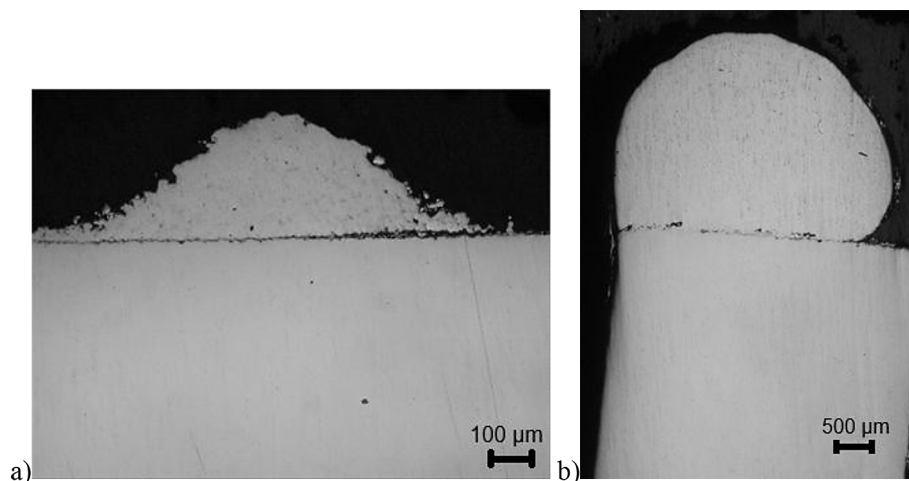


Figure 9. General view of sprayed (a) and remelted (b) Inconel 82 coating (before etching)

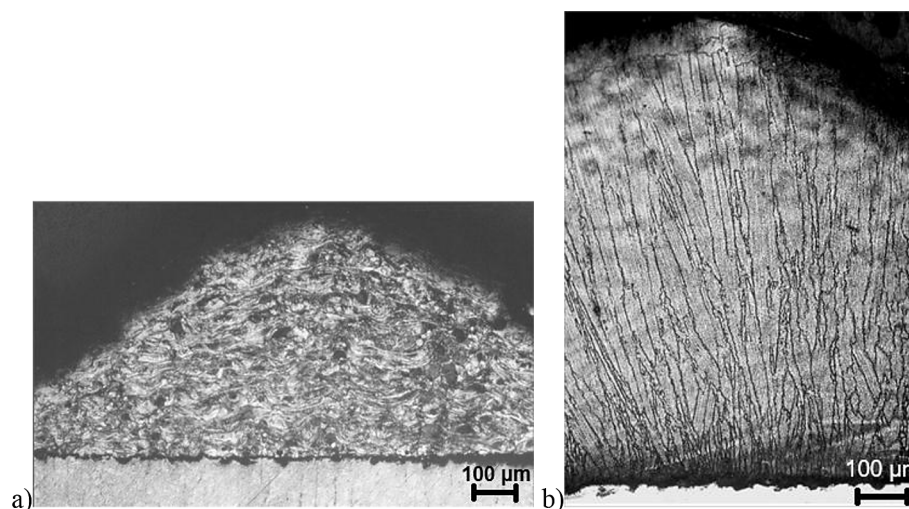


Figure 10. General view of sprayed (a) and remelted (b) Inconel 82 coating (after etching)

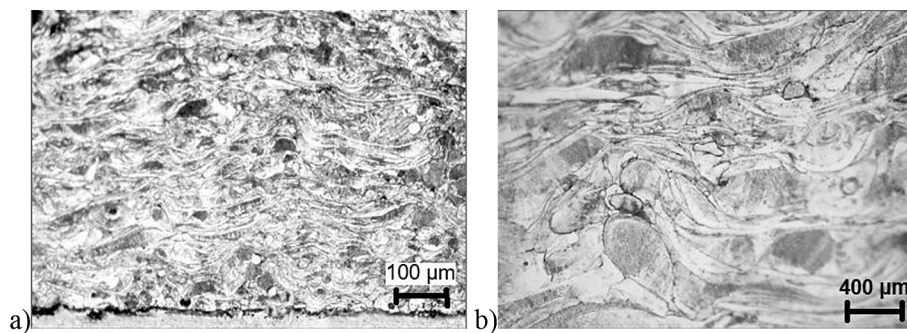


Figure 11. Microstructure of microplasma wire coating from Inconel 82 at the steel sample end face

in the deposited metal. Complete recrystallization of the metal took place after laser processing. Crystallization begins from the zone of fusion with the base metal in the form of fine elongated dendrites 3–5 μm wide and 25–35 μm long (Fig. 10,b). Towards the middle of the remelted bead the dendrites coalesce into coarser ones (Fig. 12,a), extending to almost the entire bead height. Formation of an edge zone leads to another crystallization type (Fig. 10,b). Finer equiaxed grains of 50–120 μm size are observed in it. Edge zone width varies from 20 μm near the base, to 150 μm in the highest zone of the bead. Average microhardness of the deposited metal is equal to 255 ± 29 HV, and that of the base metal is 354 ± 30 HV. A HAZ 100–200 μm thick with higher microhardness of 550 ± 30 HV is observed in the zone of bonding of the remelted bead with the base metal (Fig. 12,b). Thus, deposited bead microhardness increased by 17% after laser processing.

Increased microhardness of the HAZ indicates the formation of carbides in it under the

action of high-speed laser heating-cooling. The size of the HAZ is not critical from the standpoint of the threat of microcracks. Detailed studies of the transition zone between the remelted coating and the substrate showed the presence of their fusion with the formation of a solid solution of iron and nickel.

DISCUSSION

In previous calculations performed on the basis of dependencies 1–3 using the finite element method, the parameters of microplasma spraying and laser remelting modes were selected, based on allowing for the heat input into the base metal and into the previously deposited bead from Inconel 82 alloy. Further experiments were conducted without additional correction of the selected modes (current 30–40 A at voltage 40 V, deposition speed 100 mm/min). It was

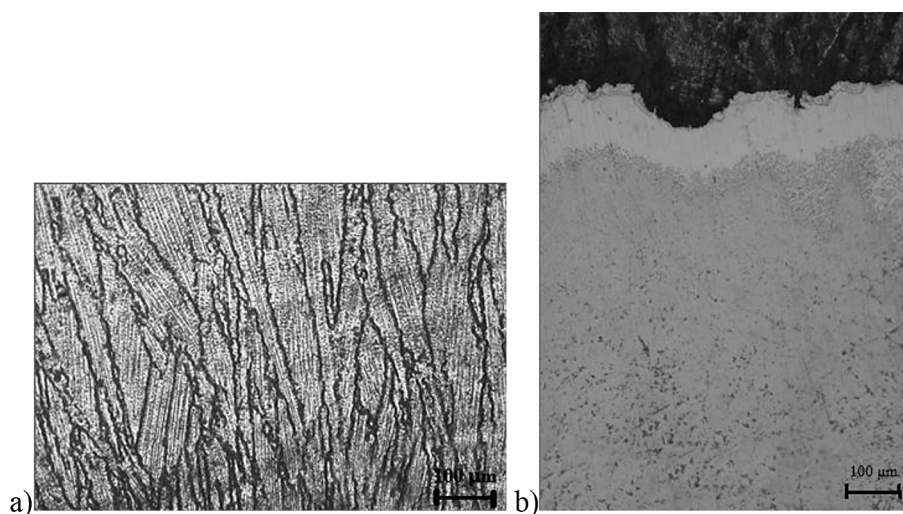


Figure 12. Microstructure of microplasma wire coating from Inconel 82 remelted by the laser (a), and zone of HAZ fusion with the base metal (b)

determined that at microplasma spraying the base metal was heated to 180–200 °C. Obtained result is indicative of calculation accuracy of the order of 12–20%. At further laser remelting of the 1.2 mm high bead from Inconel 82 alloy deposited on the base metal the total penetration depth was 1.4 mm. This value practically coincides with the calculated values. On the whole, the accuracy of preliminary calculations can be assessed as the one which provides an up to 20% error. The conducted modeling provided less accuracy than that described in papers [11, 24], but at the same time it is much easier to perform and requires less time and resources.

In plasma spraying processes, the coating growth rate parameter determines the productivity of the technology. It was found that in the case of microplasma spraying of Inconel 82 alloy this parameter was 1 mm of coating height / 1 cm of narrow path length / 1 min of spraying process duration. For the technology of microplasma spraying with small diameter wires (of the order of 0.2–0.4 mm) such a value is acceptable, and it is indicative of rather high productivity. Maximal height of the coating was in the range of 1.0–1.2 mm for 3.4 m/min feed rate of sprayed Inconel 82 wire 0.3 mm in diameter, and 1.7–1.9 mm for 5.8 m/min rate (modes 1 and 2, respectively, Table 3). Coating up to 1.2 mm high of the width, which was guaranteed to cover the sample width, was sprayed on the surface of 3 mm wide samples. As shown by experiments on spraying of 6 mm wide samples in the same mode, bead width was 4 mm. Coatings up to 1.9 mm high were sprayed on the surface of 6 mm thick samples, their width being 4–5 mm.

To determine the width of sprayed paths, several 1 mm high paths were deposited on 50 mm wide surface of 50 × 50 × 10 mm samples in modes 1 i 2 (Table 3). Results of measurement of the total width of the narrow path section showed that in the case of spraying Inconel 82 it varies in the range from 4.8–5.0 mm to 9.7–9.8 mm. The difference when spraying of 3 mm and 6 mm wide samples is insignificant. Considering, however, that the distribution of the material of spraying spot of the coating is described by Gauss's law, it can be assumed that the useful area of the spot which contains 95% of the total volume of sprayed material corresponds to a diameter of 3.2–6.5 mm.

Mechanical testing of the strength of adhesion of the deposited layers of Inconel 82 alloy

to the steel base was conducted by the standard adhesive procedure using MTS 318.25 machine. It was determined that the adhesion strength is of the order of 20–30 MPa, which is an insufficiently high value for the tasks of equipment reconditioning, usually arising in nuclear power engineering, aerospace and textile industry, etc. Note that the obtained adhesion indices are not the best. Thus, in paper [21], approximately twice as good indices are given. For this, the authors propose to improve the preparation of the substrate. In our opinion, this will increase the time and cost of industrial production of the coated part. Therefore, in order to increase this value, it was rational to use laser remelting of sprayed coatings with their fusion with the base.

During electrolytic etching of the sprayed and remelted samples in 20% aqueous solution of ammonium sulphate (chloride) it was found that for high-quality detection of Inconel 82 alloy structure the etching time differed. For sprayed samples it was 4 s, and for remelted samples it was 6 s. This indirect characteristic may indicate an increase in corrosion resistance of Inconel 82 alloy after laser processing. Such an increase in corrosion resistance can be equal approximately up to 50%. Typically, corrosion resistance tests are carried out using special methods, for example, in a molten salt environment, as described in paper [26]. Unfortunately, the authors of this work did not have the opportunity to conduct such detailed research and limited themselves to the described evaluation approach.

Laser remelting was performed on coatings sprayed on the end faces of 3 mm wide samples (sample size was 50 × 3 × 10 mm). Deposited beads of Inconel 82 alloy of width ~13% smaller than those produced by microplasma spraying were formed as a result of experiments on laser processing. A small increase in coating height (by 5–15%) was also observed. This effect is attributable to the action of surface tension forces and increase in the sprayed layer density during their remelting. It was found that laser remelting of microplasma coatings from Inconel 82 wire allows forming a deposited bead without internal porosity, which has a strong metallurgical bond with the base metal. The obtained result is indirectly confirmed by the results of such papers as [23, 24, 26]. To create such a bond, the substrate metal is remelted to the depth of the order of 200 μm, a transition zone of 5–10 μm or greater width is

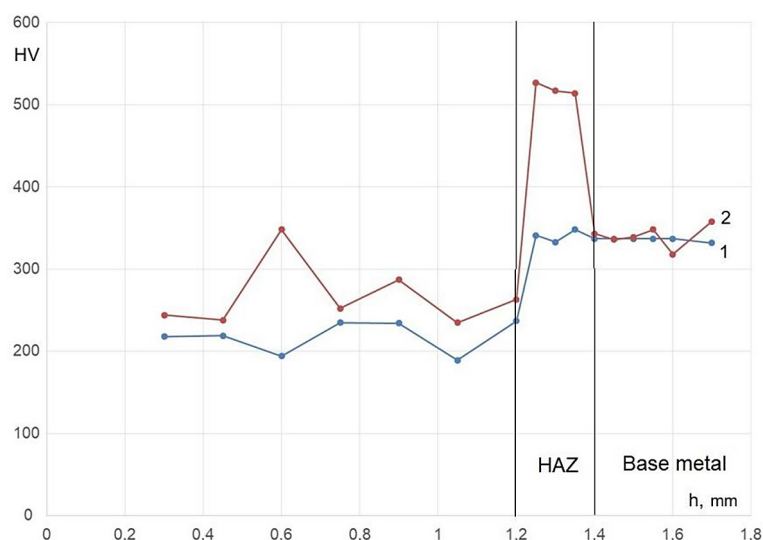


Figure 13. Distribution of microhardness HV over depth h [mm] of processed sample of «Inconel 82 alloy – 24CrMoV55 steel»: 1 – microhardness in the sprayed layer of 82 alloy; 2 – microhardness in the remelted bead of Inconel 82 alloy

formed, depending on the process parameters, and a HAZ of up to 100–200 μm size forms in the base metal below the transition zone. In individual cases oxide inclusions were detected in the remelted metal of the peripheral regions of the formed deposited bead, where the impact of laser radiation was minimal. It should be noted that the selected laser remelting modes made it possible to avoid the effect of peeling of remelted coatings described in paper [33].

Comparison of the results of microhardness measurement of the sprayed and remelted layers of Inconel 82 alloy showed an increase in the remelted bead hardness by up to 17% (Fig.13). In particular, the authors of paper [28] noticed this effect. This effect is attributable to formation of a certain grain structure of the metal and absence of burnout of elements forming the hard phases, during laser remelting. The increase in the microhardness of the plasma coating after laser remelting is also discussed in papers [31, 32]. However, for alloy Inconel 82 this effect was discovered for the first time. An overall tendency is hardness reduction after laser processing, which is associated with burnout of hard phases under the impact of focused laser radiation. In our case, remelting was performed by defocused radiation, which promoted a lowering of its power density to $4.3 \cdot 10^4 \text{ W/cm}^2$. At such values of radiation power density, no burnout of alloy elements occurs.

Friction machine 2070 SMT-1 was used to conduct wear resistance testing by “disc – pad”

scheme. The tests were conducted similarly to those described in work [4]. Testing showed that wear resistance of remelted layers of Inconel 82 alloy exceeds the wear resistance of the layers produced by microplasma spraying by 20–40%. It can be assumed that this is promoted by the fine-grained structure of Inconel 82 alloy produced during laser remelting, as well as by the above-described increase in its microhardness.

Thus, laser processing of Inconel 82 wire coatings produced by microplasma spraying, showed the possibility of forming remelted paths with minimal porosity and strong adhesion to the base material. Substrate material can also be melted to the depth of 0.1–0.4 μm , depending on process parameters. Formation of fine-grained structures together with microhardness increase may promote an increase in wear resistance of remelted layers of Inconel 82 alloy, compared to sprayed layers. This coincides with the conclusions of works [28, 29, 31].

The paper shows for the first time that laser remelting of a microplasma-sprayed coating made of Inconel 82 wire can increase its microhardness by ~17% (from 200–240 HV to 290–350 HV) due to the formation of fine-grained structures and the elimination of the burnout of individual alloying elements characteristic of laser processes. The technological similarity of the processes of microplasma spraying and laser remelting of sprayed layers is also shown for the first time, based on the close size of the processing spot in both processes.

CONCLUSIONS

Numerical modeling using the finite element method made it possible, by taking into account the heat input into the metal of the sprayed sample (about 100 W), to make a preliminary selection of the parameters of the microplasma wire spraying modes (current 30–40 A, process speed 100–200 mm/min) and subsequent laser remelting of the sprayed layers of Inconel 82 alloy (power 3.0 kW, spot 3.0 mm, speed 750 mm/min) with an accuracy of up to 20% acceptable for technological evaluation.

During microplasma wire spraying of Inconel 82 alloy the parameter of the coating growth rate showed high productivity, and it was equal to 1 mm of coating height/ 1 cm of narrow path length/ 1 min of spraying process duration. The useful area of the spot was equal to 3.2–6.5 mm, which is an indication of unique possibilities for narrow path deposition, that correspond to the capabilities of laser remelting without additional radiation scanning.

Laser melting of the deposited microplasma coatings from Inconel 82 alloy wire allowed producing beads without internal porosity with hardness up to ~17% (290–350 HV) higher than the hardness of the sprayed layers (200–240 HV), which is due to selection of a mode with a low power density (of the order of $4.3 \cdot 10^4$ W/cm²), which can prevent hard phase burnout. According to the results of electrolytic etching, an increase in corrosion resistance of Inconel 82 alloy of up to 1.5 times after laser remelting can be expected.

Metallographic studies of the produced results showed that microplasma wire spraying of Inconel 82 alloy allows creating a coating with fine lamellar structure with 14–20 lamelle form factor. Laser remelting of this structure leads to formation of fine elongated dendrites 3–5 µm wide and 25–35 µm long in the bead lower and middle parts, and formation of fine equiaxed grains of 50–120 µm size in the bead upper part. Wear resistance testing showed that the fine-grained structure produced during laser remelting promotes an increase in this parameter by 20–40%, compared to spraying.

Acknowledgments

The work was funded within the following programs:

- The GDAS'Project of Science and Technology Development[2020GDASYL-20200301001], China. Note: This project is a strategic project of Guangdong Provincial Academy of Sciences.

- National Key Research and Development Program of China (Project Number: 2020YFE0205300). Note: This project is part of the “One Belt, One Road” joint laboratory.

REFERENCES

1. Mauer G., Jarligo M. O., Marcano D., Rezanaka S., Zhou D., Vaße R. Recent developments in plasma spray processes for applications in energy technology. IOP Conference Series: Materials Science and Engineering, V. 181, 19th Chemnitz Seminar on Materials Engineering – 19. Werkstattstechnisches Kolloquium 16–17 March 2017, Chemnitz, Germany. 2017; 181: 012001. <https://doi.org/10.1088/1757-899X/181/1/012001>
2. Korzhyk V., Khaskin V., Grynyuk A., Shcheretskiy V., Fialko N. Comparing features in metallurgical interaction when applying different techniques of arc and plasma surfacing of steel wire on titanium. Eastern-European Journal of Enterprise Technologies, 2021; 4(12–112): 6–17. <https://doi.org/10.15587/1729-4061.2021.238634>
3. Skorokhod A., Sviridova I., Korzhik V. Structural and mechanical properties of polyethylene terephthalate coatings as affected by mechanical pretreatment of powder in the course of preparation. // Mekhanika Kompozitnykh Materialov, 1994; 30(4): 455–463. http://dx.doi.org/10.1007/978-981-19-9267-4_64
4. Volchuk V. M., Hlushkova D. B. Application of new plasma coatings for restoration of the surface of material, Functional Materials, 2024; 31(2): 205–209. <http://dx.doi.org/10.15407/fm31.02.205>
5. Weltmann K.-D., Kolb J. F., Holub M., Uhrlandt D., Šimek M., Ostrikov K. (Ken), Hamaguchi S., Cvelbar U., Černák M., Locke B., Fridman A., Favia P., Becker K. The future for plasma science and technology. Plasma Processes and Polymers, 2018; 16(1): 1800118.
6. Fialko N.M., Prokopov V.G., Meranova N.O., Korzhik V.N., Sherenkovskaya G.P. Thermal physics of gasothermal coatings formation processes. State of investigations. Fizika i Khimiya Obrabotki Materialov, 1993; 4: 83–93.
7. Fialko N.M., Prokopov V.G., Meranova N.O., Korzhik V.N., Sherenkovskaya G.P. Temperature conditions of particle-substrate systems in a gas-thermal deposition process. Fizika i Khimiya Obrabotki Materialov, 1994; 2: 59–67.
8. Kavaliauskas Ž., Kėželis R., Milieška M., Marcinauskas L., Valinčius V., Aikas M., Uscila R., Baltušnikas A., Žunda A. Influence of different plasma spraying methods on the physical properties of YSZ coatings. Surfaces and Interfaces, 2021; 24: 101120. <https://doi.org/10.1016/j.surfaces.2021.101120>

- surfin.2021.101120
9. Mrdak M. R. Characteristics of plasma spray coatings. *Vojnotehnicki glasnik* 2019; 67(1): 116–130. <https://doi.org/10.5937/vojtehg67-16558>
10. Fialko N., Dinzhos R., Sherenkovskii J., Lazarenko M., Koseva N. Establishing patterns in the effect of temperature regime when manufacturing nanocomposites on their heat-conducting properties. *Eastern-European Journal of Enterprise Technologies*, 2021; 4(5–112): 21–26. <http://dx.doi.org/10.15587/1729-4061.2021.236915>
11. Heimann R. B. The nature of plasma spraying. *Coatings*, 2023; 13(3): 622. <https://doi.org/10.3390/coatings13030622>
12. Kucuka A., Berndt C. C., Senturk U., Lima R. S. Deformation of plasma sprayed thermal barrier coatings. *Journal of Engineering for Gas Turbines and Power*, 2008; 122(3): 681–689. <https://doi.org/10.1002/9780470294635.ch80>
13. Borisov Y., Korzhyk V., Revo S. Electric and Magnetic Properties of Thermal Spray Coatings with an Amorphous Structure. *Proceedings of the International Thermal Spray Conference*, itsc1998; 687–691. <https://doi.org/10.31399/asm.cp.itsc1998p0687>
14. Borisov Yu., Kyslytsia O., Voynarovich S. (2004). Microplasma Wire Spraying. *Conference: ITSC2004*, 2004; 657–661. <https://doi.org/10.31399/asm.cp.itsc2004p0657>
15. Abdalameer N. Kh., Mazhir S. N., Salim H. M., Hammood J. Kh., Abdul Raheem Z. H. Design of micro-jet plasma system: a novel nanoparticles manufacturing method in atmospheric pressure. *Journal of Optoelectronic and Biomedical Materials*, 2022; 14(4): 203–210. <https://doi.org/10.15251/JOBM.2022.144.203>
16. Sytnykov P. A. Plasma coatings based on self-fluxing NiCrBSi alloy with improved wear resistance properties. *Journal of Mechanical Engineering – Problemy Mashynobuduvannia*, 2023; 26(3): 54–64. <https://doi.org/10.15407/pmach2023.03.054>
17. Kvasnytskyi, V., Korzhyk, V., Kvasnytskyi, V., Heorhii Mialnitsa, Dong Chunlin, Matvienko, M., Buturlia, Y. Designing brazing filler metal for heat-resistant alloys based on Ni₃Al intermetallic. *Eastern-European Journal of Enterprise Technologies*, 2020; 6(12): 6–19. <http://dx.doi.org/10.15587/1729-4061.2020.217819>
18. Łatka L. Thermal barrier coatings manufactured by suspension plasma spraying – a review. *Advances in Materials Science*, 2018; 18(3): 95–117. <http://dx.doi.org/10.1515/adms-2017-0044>
19. Prokopov V., Fialko N., Sherenkovskaya G. P., Yurchuk V., Borisov Y., Murashov A., Korzhik V. Effect of the coating porosity on the processes of heat transfer under, gas-thermal atomization. *Poroshkovaya Metallurgiya*, 1993; (2), 22–26.
20. Odhiambo J. G., Li W. G., Zhao Y. T., Li C. L. Porosity and its significance in plasma-sprayed coatings. *Coatings*, 2019; 9(7): 460. <https://doi.org/10.3390/coatings9070460>
21. Abhinav, H. K. Kustagi, A. R. Shankar Adhesion Strength of Plasma Sprayed Coatings—A Review. In: Reddy, A., Marla, D., Simic, M., Favorskaya, M., Satapathy, S. (eds) *Intelligent Manufacturing and Energy Sustainability. Smart Innovation, Systems and Technologies*, 2020; 169. Springer, Singapore. https://doi.org/10.1007/978-981-15-1616-0_8
22. Skorokhod A. Z., Sviridova I. S., Korzhik V. N. The effect of mechanical pretreatment of polyethylene terephthalate powder on the structural and mechanical properties of coatings made from it. *Mechanics of Composite Materials*, 1995; 30(4): 328–334.
23. Wang K. L., Zhu Y. M., Steen W. M. Laser remelting of plasma sprayed coatings. *Journal of Laser Applications*, 2000; 12: 175–178. <https://doi.org/10.2351/1.521930>
24. Li C., Han X., Zhang D., Gao X., Jia T. Quantitative analysis and experimental study of the influence of process parameters on the evolution of laser cladding. *Journal of Adhesion Science and Technology*, 2021; 36(17): 1894–1920. <https://doi.org/10.1080/1694243.2021.1991142>
25. Gu Y., Xu Y., Shi Y., Feng C., Volodymyr K. Corrosion resistance of 316 stainless steel in a simulated pressurized water reactor improved by laser cladding with chromium. *Surface and Coatings Technology*, 2022; 441: 128534. <https://doi.org/10.1016/j.surfcoat.2022.128534>
26. Gu Y., Zhang W., Xu Y., Shi Y., Volodymyr K. Stress-assisted corrosion behaviour of Hastelloy N in FLiNaK molten salt environment. *npj Materials Degradation*, 2022; 6(1): 90. <https://doi.org/10.1038/s41529-022-00300-x>
27. Li C., Wang Y., Guo L., He J. Laser remelting of plasma-sprayed conventional and nanostructured Al₂O₃ – 13 wt.%TiO₂ coatings on titanium alloy. *Journal of Alloys and Compounds*, 2010; 506(1): 356–363. <https://doi.org/10.1016/j.jallcom.2010.06.207>
28. Cao Y., Yuan C., Zhang Y., Ma J. Laser cladding performance and process parameter optimization for Fe90 alloy. *Metals*, 2024; 14(12): 1432. <https://doi.org/10.3390/met14121432>
29. Afzal M., Nusair Khan A., Ben Mahmud T., Khan T.I., Ajmal M. Effect of laser melting on plasma sprayed WC-12wt.%Co coatings. *Surface and Coatings Technology*, 2015; 266: 22–30. <https://doi.org/10.1016/j.surfcoat.2015.02.004>
30. Jing H., Yu S., Gang, Z., Volodymyr K. Minimizing defects and controlling the morphology of laser welded aluminium alloys using power modulation-based laser beam oscillation. J.

- Manufacturing Processes, 2022; 83, 49–59. <https://doi.org/10.1016/j.jmapro.2022.08.031>
31. Ge Y., Wang W., Wang X., Cui Z., Xu B. Study on laser surface remelting of plasma-sprayed Al-Si/1wt% nano-Si₃N₄ coating on AZ31B magnesium alloy. *Applied Surface Science*, 2013; 273: 122–127. <https://doi.org/10.1016/j.apsusc.2013.01.204>
32. Zhou Y., Xu L., Zheng H., Wang D. Surface modification of plasma spraying Al₂O₃–13 wt% TiO₂ coating by laser remelting technique. *Materials Research Express*, 2022; 9: 056401. <https://doi.org/10.1088/2053-1591/ac6a49>
33. Guo K., Wang Y., Chen R. et al. Laser-induced layers peeling of sputtering coatings at 1064 nm wavelength. *Scientific Reports*, 2021; 11: 3783. <https://doi.org/10.1038/s41598-020-80304-2>
34. Dworak J., Dymek S., Kalembe-Rec I., Wrona A., Kustra K., Lis M. Laser remelting of Ni-Cr-Re plasma spraying coating. Conference: METAL 2020; 2694–9296: 846–851. <https://doi.org/10.37904/metal.2020.3562>
35. Liao J., Zhang L., Peng C., Jia Y., Wang G., Wang H., An X. Fabrication of Ni–Cu–W graded coatings by plasma spray deposition and laser remelting. *Materials*, 2022; 15(8): 2911. <https://doi.org/10.3390/ma15082911>
36. Laik A., Chakravarthy D.P., Kale G.B. On characterisation of wire-arc-plasma-sprayed Ni on alumina substrate. *Materials Characterization*, 2005; 55(2): 118–126. <https://doi.org/10.1016/j.matchar.2005.04.001>
37. Kelkar M., Heberlein J. Wire-arc spray modeling. *Plasma Chemistry and Plasma Processing*, 2002; 22: 1–25. <https://doi.org/10.1023/A:1012924714157>
38. Song Z., Li H. Plasma spraying with wire feeding: A facile route to enhance the coating/substrate interfacial metallurgical bonding. *Coatings*, 2022; 12(5): 615. <https://doi.org/10.3390/coatings12050615>
39. Domokos I., Pálkás S. Application of laser remelting technology in the case of cultivator tines. *Coatings*, 2024; 14(5): 637. <https://doi.org/10.3390/coatings14050637>
40. Song Z., Li H. Plasma spraying with wire feeding: A facile route to enhance the coating/substrate interfacial metallurgical bonding. *Coatings*, 2022; 12(5): 615. <https://doi.org/10.3390/coatings12050615>
41. Yung T.-Y., Chen T.-C., Tsai K.-C., Lu W.-F., Huang J.-Y., Liu T.-Y. thermal spray coatings of Al, ZnAl and inconel 625 alloys on SS304L for anti-saline corrosion. *Coatings*, 2019; 9(1): 32. <https://doi.org/10.3390/coatings9010032>
42. Adam Khan M., Sundarrajan S., Natarajan S. Influence of plasma coatings on Inconel 617 for gas turbine applications. *Surface Engineering*, 2014; 30(9): 656–661. <https://doi.org/10.1179/1743294414Y.0000000029>
43. Panneerselvam G., Raju S., Jose R., Sivasubramanian K., Divakar R., Mohandas E., Antony M.P. A study on the thermal expansion characteristics of Inconel-82® filler wire by high temperature X-ray diffraction. *Materials Letters*, 2004; 58(1–2): 216–221. [https://doi.org/10.1016/S0167-577X\(03\)00448-8](https://doi.org/10.1016/S0167-577X(03)00448-8)
44. Merino-Millan D., Múnez C. J., Garrido-Maneiro M. Á., Poza P. Alternative low-power plasma-sprayed inconel 625 coatings for thermal solar receivers: Effects of high temperature exposure on adhesion and solar absorptivity. *Solar Energy Materials and Solar Cells*, 2022; 245: 111839. <https://doi.org/10.1016/j.solmat.2022.111839>
45. Kumar S., Kumar R. Influence of processing conditions on the properties of thermal sprayed coating: a review, *Surface Engineering*, 2021; 37(11): 1339–1372. <https://doi.org/10.1080/02670844.2021.1967024>
46. Qadir D., Sharif R., Nasir R., Awad A., Mannan H. A. A review on coatings through thermal spraying, *Chemical Papers*, 2023; 1: 71–91. <https://doi.org/10.1007/s11696-023-03089-4>
47. Fialko, N., Dinzhos, R., Sherenkovskii, J. Mankus, I., Nedbaievska, L. Establishment of regularities of influence on the specific heat capacity and thermal diffusivity of polymer nanocomposites of a complex of defining parameters. *Eastern-European Journal of Enterprise Technologies*, 2021; 6(12(114)): 6–12. <https://doi.org/10.15587/1729-4061.2021.245274>
48. Anand M., Das A. K. Grain refinement in wire-arc additive manufactured inconel 82 alloy through controlled heat input. *Journal of Alloys and Compounds*, 2022; 929: 166949. <https://doi.org/10.1016/j.jallcom.2022.166949>
49. Panneerselvam G., Raju S., Jose R., Sivasubramanian K., Divakar R., Mohandas E., Antony M.P. A study on the thermal expansion characteristics of Inconel-82® filler wire by high temperature X-ray diffraction. *Materials Letters*, 2004; 58(1–2): 216–221. [https://doi.org/10.1016/S0167-577X\(03\)00448-8](https://doi.org/10.1016/S0167-577X(03)00448-8)
50. Han Y.R., Zhang C.H., Cui X., Zhang S., Zhang J.B., Liu Y. The formability and microstructure evolution of 24CrNiMo alloy steel fabricated by selective laser melting. *Vacuum*, 2020; 175: 109297. <https://doi.org/10.1016/j.vacuum.2020.109297>
51. Zhou H., Liu Z., Luo L. Microstructural characterization of shrouded plasma-sprayed titanium coatings. *Journal of Manufacturing and Materials Processing*, 2019; 3(1): 4. <https://doi.org/10.3390/jmmp3010004>
52. Kaiming W., Yulong L., Hanguang F., Yongping L., Zhenqing S., Pengfei M. A study of laser cladding NiCrBSi/Mo composite coatings. *Surface Engineering*, 2018; 34(4): 267–275. <https://doi.org/10.1080/>

- 02670844.2016.1259096
53. Standard Guide for Preparation of Metallographic Specimens. Copyright © ASTM International, 100 Barr Harbor Drive, PO Box C700, West Conshohocken, 2011; 19428–2959. United States. <https://doi.org/10.1520/E0003-11>
 54. Akca E., Trgo E. Metallographic procedures and analysis – A review. *Periodicals of Engineering and Natural Sciences (PEN)*, 2015; 3(2): 9–11. <https://doi.org/10.21533/pen.v3i2.51>
 55. Fox G. R., Liang H. Wear mode comparison of high-performance Inconel alloys. *Journal of Tribology*, 2010; 132(2). <https://doi.org/10.1115/1.4001170>
 56. Pogonyshv V.A., Torikov V.E., Mokshin I.A., Pogonysheva D.A., Boiko A.A. Leveling Out the Effect of Sample Runouts on Wear when Testing on the SMT-1 Friction Machine, ICMTMTE 2021, MATEC Web of Conferences, 2021; 346: 03042. <https://doi.org/10.1051/mateconf/202134603042>
 57. Khaskin V.Yu. Calculation and experimental method for determining the parameters of laser cladding processes. *Science and Innovations*, 2012; 8(6): 5–16.
 58. Xv Y., Sun Y., Zhang Y. Prediction method for high-speed laser cladding coating quality based on random forest and adaboost regression analysis. *Materials (Basel)*, 2024; 17(6): 1266. <https://doi.org/10.3390/ma17061266>
 59. Korzhik, V.N. Theoretical analysis of amorphization conditions for metallic alloys under gas-thermal spraying. III. Transformations in the amorphized alloy underbuilding-up of coatings // *Poroshkovaya Metallurgiya* 1992; (11): 47–52.
 60. Zhilkashinova A., Abilev M., Zhilkashinova A. Microplasma-sprayed V2O5/C double-layer coating for the parts of mini-hydropower systems. *Coatings*, 2020; 10(8): 725. <https://doi.org/10.3390/coatings10080725>
 61. Fialko N.M., Prokopov V.G., Meranova N.O., Korzhik V.N., Sherenkovskaya G.P. Temperature conditions of particle-substrate systems in a gas-thermaldeposition process. *Fizika i Khimiya Obrabotki Materialov*, 1994; 2 : 59–67.
 62. Fauchais P., Vardelle A. Innovative and emerging processes in plasma spraying: from micro- to nano-structured coatings. *Journal of Physics D: Applied Physics*, 2011; 44: 194011. <https://doi.org/10.1088/0022-3727/44/19/194011>
 63. Fialko N., Dinzhos R., Sherenkovskii J. Korzhyk V., Lazarenko M., Makhrovskiy V. Influence on the thermophysical properties of nanocomposites of the duration of mixing of components in the polymer melt. *Eastern-European Journal of Enterprise Technologies*, 2022; 2(5–116): 25–30. <https://doi.org/10.15587/1729-4061.2022.255830>